



HAL
open science

Minimizing electromagnetic exposure for wireless mm-size neural implants

Denys Nikolayev, Anja Skrivervik, Wout Joseph, Luc Martens, Ronan Sauleau, Maxim Zhadobov

► **To cite this version:**

Denys Nikolayev, Anja Skrivervik, Wout Joseph, Luc Martens, Ronan Sauleau, et al.. Minimizing electromagnetic exposure for wireless mm-size neural implants. BioEM 2020, Jun 2020, Oxford, United Kingdom. hal-03386406

HAL Id: hal-03386406

<https://hal.science/hal-03386406>

Submitted on 21 Oct 2021

HAL is a multi-disciplinary open access archive for the deposit and dissemination of scientific research documents, whether they are published or not. The documents may come from teaching and research institutions in France or abroad, or from public or private research centers.

L'archive ouverte pluridisciplinaire **HAL**, est destinée au dépôt et à la diffusion de documents scientifiques de niveau recherche, publiés ou non, émanant des établissements d'enseignement et de recherche français ou étrangers, des laboratoires publics ou privés.

Minimizing electromagnetic exposure for wireless mm-size neural implants

Denys Nikolayev¹, Anja Skrivervik², Wout Joseph³, Luc Martens³, Ronan Sauleau¹ & Maxim Zhadobov¹

¹*Univ Rennes, CNRS, IETR (Institut d'Électronique et de Télécommunications de Rennes) UMR–6164, FR-35000 Rennes, France*

²*Microwaves and Antennas Group (MAG), EPFL, CH-1015 Lausanne, Switzerland*

³*INTEC – WAVES, imec / Ghent University, BE-9052 Ghent, Belgium*

Keywords: Dosimetry (computational), RF/Microwaves, Completed (unpublished)

Wireless neural interfaces provide major leap capabilities for neurotechnology by removing hazardous and bulky percutaneous links. This study addresses for the first time the radio frequency (RF) electromagnetic (EM) exposure of mm-sized neural implant antennas in the frequency range from 100 MHz to 4 GHz. The results demonstrate the existence of mode-dependent optimal radiating conditions that minimize the total dissipated power and Specific Absorption Rate (SAR) for a given input power. Peak SAR is in average 3.7 times lower for the magnetic source than for the electric one. This study provides decision-making insights into how to design EM-safe and efficient antennas for mm-sized wireless implants.

Introduction

Neural interfaces allow us to study the brain via mapping, assisting, augmenting, and repairing cognitive or sensory-motor functions [Jackson and Zimmermann, 2012]. In addition, the emerging electroceuticals aim individual neural circuits that regulate the physiological processes to treat a wide range of illnesses [Famm et al., 2013]. High-resolution deep brain leads still require percutaneous links that presents high clinical risks, restrict mobility, and does not scale for large brain coverage. Wireless implants mitigate these drawbacks and therefore enable a major leap in neurotechnology [Borton et al., 2013]. Wireless links based on radio- frequency antennas currently provide highest data rates and power efficiencies [Poon, 2014]. For a given

antenna input power, the electromagnetic exposure of brain tissues depends on the antenna type and operating frequency [Nikolayev et al., 2018]. Whereas the exposure analysis of the realistic body-implanted antennas has been reported, there is a lack of systematic knowledge on the exposure of the brain tissues by mm-sized antennas. This study addresses this issue by studying the frequency dependent power dissipation and SAR of fundamental mm-sized magnetic and electric antennas in the frequency range from 100 MHz to 4 GHz. Minima of power absorption and SAR are identified with respect to the antenna types and operating frequency.

Methods

EM exposure by mm-size neural implant antennas is analyzed in the stratified spherical phantom based on [Nikolayev et al., 2019b; Skrivervik et al., 2019] that represents human head tissues (Figure 1). The outer diameter of the phantom is 100 mm, and the source is centered inside of the sphere. Despite larger average head dimensions, this diameter is sufficient taking into account local absorption of the radiated power around the implant [Nikolayev et al., 2019c]. Each layer is assumed homogeneous. The skin thickness is 2 mm, the subcutaneous fibroadipose tissue (modeled as fat) is 4 mm [Kuster et al., 2000], and the skull (cortical bone) is 6.8 mm (thickness averaged from [Li et al., 2007]). Each tissue is assigned dispersive EM properties based on four-region Cole–Cole model based on [Gabriel et al., 1996]. The dura and the brain are modeled as a single layer since their EM properties are similar. Brain tissue was modeled as gray matter because of its higher conductivity than white matter.

The antenna is modeled as either an equivalent \mathbf{E} -coupled source radiating TM_{10} mode or as a magnetic \mathbf{B} -coupled (TE_{10}) source. The sources are modeled as $\mathbf{J}_s(r, \varphi, z)$ distribution over a parametrized cylindrical surface enclosed in a capsule volume (Figure 1). The validity of this model is discussed in [Nikolayev et al., 2019b]. The diameter of the source is $D = 1.27$ mm corresponding to a Medtronic lead for DBS [Medtronic, 2020], the length is $L = 5$ mm, and the insulation thickness 100 μm (modeled as silicone with $\epsilon_r = 3$).

Radiated EM field is governed by the inhomogeneous wave equation. In terms of the time-harmonic electric field \mathbf{E} (time variations of the form $e^{j\omega t}$), it is expressed as $\nabla^2 \mathbf{E} = j\omega\mu\mathbf{J}_s + j\omega\mu\sigma\mathbf{E} - \omega^2\mu\epsilon\mathbf{E}$, where \mathbf{J}_s is the source electric current density [Jackson, 1999]. It is assumed that the implant is composed of nonmagnetic materials (i.e. $\mu \equiv \mu_0$). Taking into account axial symmetry for the formulated problem $\mathbf{E}(r, \varphi, z) = \mathbf{E}(r, z)\exp(-jm\varphi)$ (see Figure 1), the model order is reduced to \mathbf{R}^2 . The current distributions on the surface of equivalent sources are defined as $\mathbf{J}_{s, \text{TE}} = [0 \ 1 \ 0]$ $\text{A}\cdot\text{m}^{-2}$ for the TE_{10} source and as $\mathbf{J}_{s, \text{TM}} = [0 \ 0 \ \cos(\pi z/L)]$ $\text{A}\cdot\text{m}^{-2}$ for the TM_{10} . The supplied, radiated, and dissipated powers are calculated using the Poynting theorem [Jackson, 1999]. Local $\text{SAR} = \sigma|\mathbf{E}|^2/\rho$ is calculated considering the average density of gray matter $\rho = 1045$ $\text{kg}\cdot\text{m}^{-3}$ [Hasgall et al., 2018]. The problem is solved with a finite-element method in \mathbf{R}^2 using an axisymmetric time-harmonic formulation [Karban et al., 2013].

Results and Discussion

First, we analyze the effect of operating frequency and source type on power absorption in tissues from 100 MHz to 4 GHz. The normalized dissipated power given in Figure 2a demonstrates a distinctive minimal absorption within the frequency range of 1–1.5 GHz for both source formulations. This optimum is a result of a trade-off between the attenuation due to the dielectric losses and mismatch losses caused by the high wave-impedance contrast between media [Nikolayev et al., 2018]. Magnetic sources show significantly lower relative power absorption: 97.8% of the minimal absorbed power vs 99.3% for the electric ones. Note that for the larger dimensions of the antenna (approx. $L > 1$ cm) this trend reverses, and the electric sources yield lower absorbed power than the magnetic ones (see [Nikolayev et al., 2019a]).

Concerning the peak local SAR, mm-sized implants would benefit from magnetic source types as well. Figure 2b shows the frequency-dependent SAR normalized by the supplied power. Clearly, magnetic sources are preferable independently of the operating frequency. Peak SAR is 3.7 times lower in average over the considered frequency range for the magnetic source than for the electric one. As for the total dissipated power, an optimal frequency range could be identified yielding a local-SAR minimum within the range of 2.5–3.5 GHz. Finally, Figure 3 shows the distributions of local SAR induced by both source types operating at

400 MHz, 1.4, 2.45, and 4 GHz. At 400 MHz, the electric source yields a high gradient of SAR with maxima localized at the edges of the source. The magnetic source has its maximum SAR at the center of the source due to the maximum induced electric field in this region. Higher operating frequencies have moderate effect on the SAR distribution of the electric source; only the normalized peak SAR varies according to Figure 2b. In contrast, the SAR homogeneity increases with the frequency for the magnetic source.

Conclusion

This study addressed the electromagnetic exposure of the brain tissues by wireless mm-sized implants. The results revealed that the exposure could be minimized by appropriately choosing the antenna type and operating frequency. For the considered antenna dimensions of 1.27×5 mm, magnetic sources such as loop antennas yield significantly lower power dissipation levels and SAR than the electric ones (such as dipoles, monopoles, patches). Peak SAR was analyzed instead of the averaged SAR considering the ultra-miniature source dimensions. In addition, such small sources produce extremely localized SAR distributions. Being in direct vicinity to neurons, it is important to minimize the local SAR peak instead of the averaged SAR in order to minimize the probability of locally induced thermal effects.

To the best of authors' knowledge, the obtained frequency-dependent fundamental limits of the minimum relative power absorption level and normalized peak SARs were computed for the first time. These results provide decision-making insights into how to design EM-safe and efficient antennas for mm-sized wireless implants.

Acknowledgement

This study was supported by the the Labex CominLabs PKSTIM project.

References

- Borton DA, Yin M, Aceros J, Nurmikko A. 2013. An implantable wireless neural interface for recording cortical circuit dynamics in moving primates. *J. Neural Eng.* 10:026010.
- Famm K, Litt B, Tracey KJ, Boyden ES, Slaoui M. 2013. Drug discovery: A jump-start for electroceuticals. *Nature* 496:159–161.
- Gabriel S, Lau RW, Gabriel C. 1996. The dielectric properties of biological tissues: II. Measurements in the frequency range 10 Hz to 20 GHz. *Phys. Med. Biol.* 41:2251–2269.
- Hasgall PA, Gennaro FD, Baumgartner C, Neufeld E, Lloyd B, Gosselin MC, Payne D, Klingensböck A, Kuster N. 2018. IT'IS Database for thermal and electromagnetic parameters of biological tissues. Version 4.0, DOI: 10.13099/VIP21000-04-0. itis.swiss/database.
- Jackson A, Zimmermann JB. 2012. Neural interfaces for the brain and spinal cord—restoring motor function. *Nature Reviews Neurology* 8:690–699.
- Jackson JD. 1999. *Classical Electrodynamics* 3rd ed. Hoboken, NJ: John Wiley & Sons.
- Karban P, Mach F, Kús P, Pánek D, Doležel I. 2013. Numerical solution of coupled problems using code Agros2D. *Computing* 95:381–408.
- Kuster N, Santomaa V, Drossos A. 2000. The dependence of electromagnetic energy absorption upon human head tissue composition in the frequency range of 300-3000 MHz. *IEEE Trans. Microwave Theory Techn.* 48:1988–1995.
- Li H, Ruan J, Xie Z, Wang H, Liu W. 2007. Investigation of the critical geometric characteristics of living human skulls utilising medical image analysis techniques. *Int. J. Veh. Saf.* 2:345.
- Medtronic. 2020. Medtronic Lead Kit for Deep Brain Stimulation. <http://www.medtronic.com/downloadablefiles/UC199901079bEN.pdf>.
- Nikolayev D, Joseph W, Skrivervik AK, Zhadobov M, Martens L, Sauleau R. 2019a. Dielectric-loaded conformal microstrip antennas for versatile in-body applications. *IEEE Antenn. Wireless Propag. Lett.* 18:2686–2690.
- Nikolayev D, Joseph W, Zhadobov M, Sauleau R, Martens L. 2019b. Optimal radiation of body-implanted capsules. *Phys. Rev. Lett.* 122:108101.

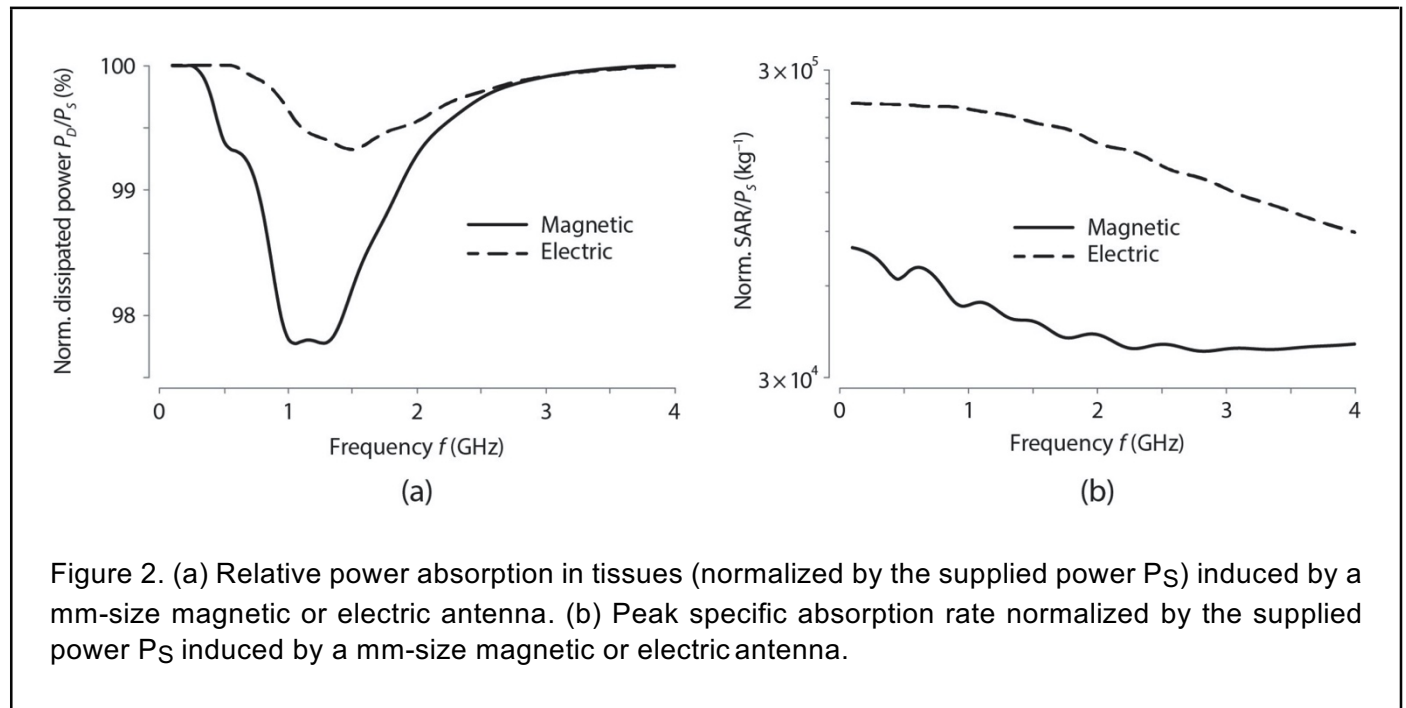
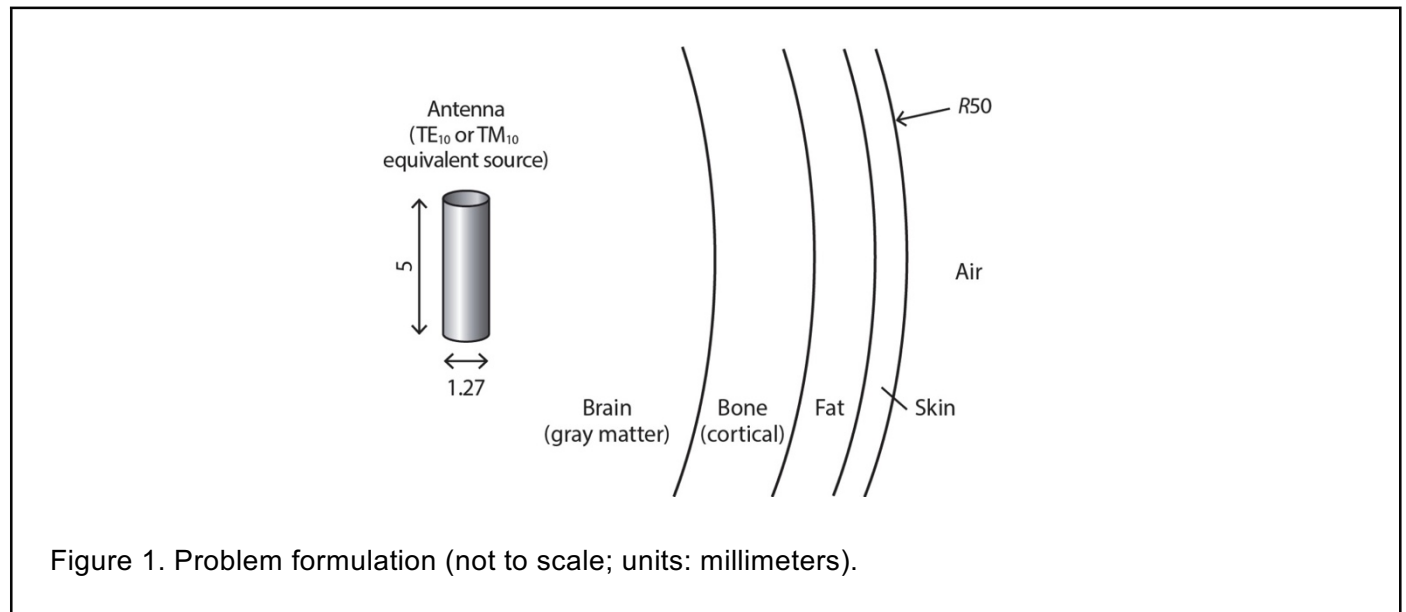
Nikolayev D, Joseph W, Zhadobov M, Sauleau R, Martens L, Skrivervik AK. 2019c. Exposure assessment of body-implanted capsules in the 100-MHz–5-GHz range. In: Proc. BioEM 2019. Montpellier, France. p. 63–67.

Nikolayev D, Zhadobov M, Karban P, Sauleau R. 2018. Electromagnetic radiation efficiency of body-implanted devices. Phys. Rev. Applied 9:024033.

Poon ASY. 2014. Miniaturized Biomedical Implantable Devices. In: Implantable Bioelectronics. Weinheim, Germany: Wiley-VCH. p. 45–64. <http://onlinelibrary.wiley.com/doi/10.1002/9783527673148.ch4/summary>.

Skrivervik AK, Bosiljevac M, Sipus Z. 2019. Fundamental limits for implanted antennas: Maximum power density reaching free space. IEEE Trans. Antennas Propag. 67:4978–4988.

Figures



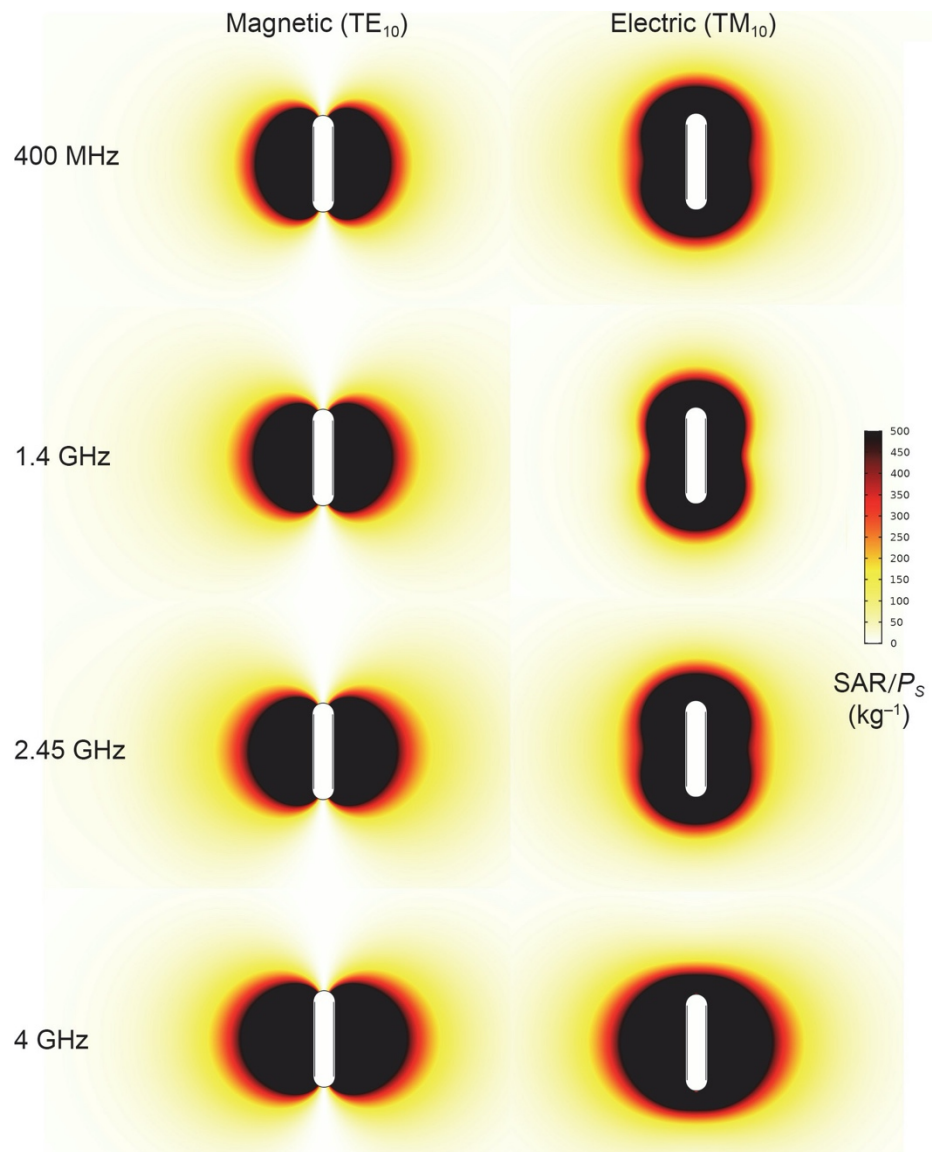


Figure 3. SAR distributions normalized by the supplied power P_S of magnetic (TE_{10}) and electric (TM_{10}) equivalent sources operating at 400 MHz, 1.4, 2.45, and 4 GHz.